Direct Observation of Adduct Formation of Alkyl and Aromatic Iodides with Cl Atoms Using Cavity Ring-Down Spectroscopy

Shinichi Enami, Takashi Yamanaka, Satoshi Hashimoto, and Masahiro Kawasaki*

Department of Molecular Engineering and Graduate School of Global Environmental Studies, Kyoto University, Kyoto 615-8510, Japan

Kenichi Tonokura

Environmental Science Center, The University of Tokyo, Tokyo 113- 0033, Japan

Received: April 19, 2005; In Final Form: May 14, 2005

The reactions of Cl atoms with RI (R = *n*-C_3H_7, *n*-C_4H_9, *cyclo*-C_6H_{11}, C_6H_5, C_6F_5, and *p*-$CH_3C_6H_4$) have been studied using cavity ring-down spectroscopy at a temperature range of 233−313 K and at 100 Torr total pressure of N_2 diluent. Visible absorption spectra of the RI−Cl adducts were recorded at 440−520 nm at 263 K. The yields of the adducts were temperature-dependent. There was no discernible reaction of the adducts in the presence of 100 Torr of O_2 at 263 K. Theoretical calculations were performed for C_4H_9I−Cl and C_6H_5I−Cl for quantitative explanation of the absorption spectra and the strength of the I−Cl bonds in the charge-transfer complexes. Evidence for the adduct formation following the reaction of Cl with C_6H_5Br was sought but not found at 440 and 520 nm.

1. Introduction

The atmospheric chemistry of iodine-containing compounds is a topic of current interest.[1] Iodine chemistry may influence radical concentrations and the destruction of ozone in the marine boundary layer.[2−4] A new mechanism for particle formation from iodine compounds in the coastal marine environment has also attracted recent attention.[5,6] Iodo- and bromo-compounds have been reported to form charge-transfer (CT) complexes with F or Cl atoms.[7−10] A Cl atom reacts with an iodo-compound to generate the CT complex via addition reaction 1a or to generate HCl via abstraction reaction 1b.

$$C_nH_{2n+1}I + Cl \rightleftarrows C_nH_{2n+1}I\text{-}Cl \quad (1a)$$

$$\rightarrow C_nH_{2n}I + HCl \quad (1b)$$

The branching ratios of these reactions depend on temperature and the nature of iodo-compounds. The branching ratio of reaction 1a for CH_3I and C_2H_5I decreases with temperature.[8,10] The visible absorption spectra of XI−Cl adducts (X = CH_3, C_2H_5, CH_2Cl, CH_2Br, and CH_2I) have been previously reported.[10] The experimentally observed spectra of CH_3I−Cl and C_2H_5I−Cl are attributable to the red wing of the $\sigma-\sigma^*$ transition. Our previous theoretical calculations show that the bonding energies of CH_3I−Cl and C_2H_5I−Cl are 59.0 and 61.7 kJ mol^{-1}, respectively. These results are consistent with the results reported by Ayhens et al.[8] In this work, we have experimentally and theoretically studied the formation of adducts of Cl atoms with aliphatic and aromatic iodides with Cl atoms.

2. Experimental Section

Since the cavity ring-down spectroscopy (CRDS) technique was introduced by O'Keefe and Deacon[11] in 1988, it has been applied widely in spectroscopic and chemical kinetic studies.[12−14] The CRDS apparatus used in the present study has been described elsewhere.[10] The system employs photolysis and probe-pulsed lasers. After the photolysis laser beam traverses the glass tube reactor, the probe laser beam is injected nearly collinear to the axis of the photolysis laser through one of two high-reflectivity mirrors (Research Electro-Optics, reflectivity > 0.999 at 440 and 488 nm). Weak absorption by Cl_2 precludes CRDS measurements below 420 nm. Light leaking from the end mirror was detected by a photomultiplier tube (Hamamatsu Photonics, R212UH) with a fast-response photomultiplier socket assembly (Hamamatsu Photonics, E5815-01) through suitable narrow band-pass filters. The decay of the light intensity was recorded using a digital oscilloscope (Tektronix, TDL-714L, 8-bit digitizer) and was transferred to a personal computer. In the presence of an absorbing species, the light intensity within the cavity is given by the expression

$$I(t) = I_0 \exp(-t/\tau) = I_0 \exp(-t/\tau_0 - \sigma n c L_R t/L_C) \quad (I)$$

where I_0 and $I(t)$ are the light intensities at time 0 and t, τ is the cavity ring-down time with photolysis laser light, τ_0 is the cavity ring-down time without photolysis laser light (typically 1.5 μs), L_R is the length of the reaction region (0.46 m), L_C is the cavity length (1.04 m), and c is the velocity of light. n and σ are the concentration and absorption cross section of the absorbing species, respectively.

The 355-nm output of a Nd^{3+}:YAG laser was used to dissociate Cl_2 to generate Cl atoms. The laser power was typically 50 mJ/pulse, at a repetition rate of 2 Hz. Shot-to-shot fluctuation of the laser power was less than 10%. Optical absorption by the RI−Cl adducts was monitored with an optical parametric oscillation laser (Spectra-Physics, MOPO-SL). A large excess of halogen compounds, $10^{14}-10^{15}$ molecule cm^{-3}, ensured that loss of Cl atoms and formation of products followed pseudo-first-order reaction conditions. When the yield of the

* To whom correspondence should be addressed. Fax: + 81-75-383-2573; e-mail: kawasaki@moleng.kyoto-u.ac.jp.

10.1021/jp0520188 CCC: $30.25
Published on Web 06/21/2005

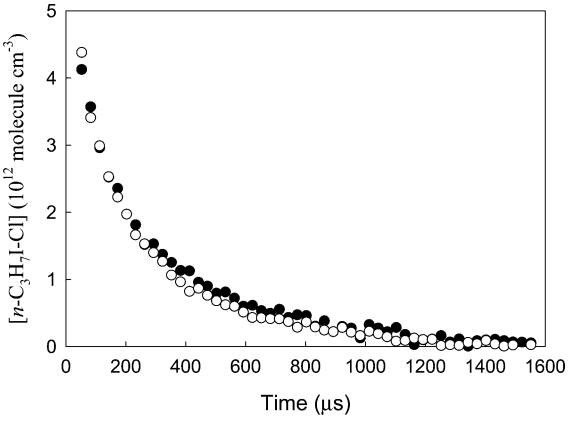

Figure 1. Typical decay time profiles of *n*-C_3H_7I-Cl at 263 K with 100 Torr of N_2 diluent (closed circle) or O_2 diluent (open circle).

adduct is unity, the maximum concentration of RI−Cl can be equated to $[Cl]_0$.

$$[RI-Cl]_{max} = [Cl]_0 \qquad (II)$$

The initial concentration of Cl atoms, $[Cl]_0$, was estimated by monitoring the chlorine oxide (ClO) produced at 273 K, using 266-nm light and a mixture of $Cl_2/O_3/O_2$. The chlorine concentrations used for this was $[Cl_2] = (1-10) \times 10^{15}$ molecule cm^{-3}. Absorption cross sections of the RI−Cl adduct were determined using the following equation and the initial concentration of Cl atoms.

$$1/\tau - 1/\tau_0 = [RI-Cl]\, \sigma\, c\, L_R/L_C \qquad (III)$$

where τ is the ring-down time in the presence of the RI−Cl adduct. The error bars of σ were estimated to be 19%.

The reaction cell consists of a Pyrex glass tube (21 mm i.d.). The temperature of the gas flow region was controlled over $T = 213-320$ K. Gas temperature difference at the entrance and exit of the flow region was <1 K. The total flow rate was adjusted so that the gas in the cell was replaced completely within the time interval of 0.5 s between photolysis laser pulses.

All reagents were obtained from commercial sources. C_6H_5I (98%), C_6F_5I (99%), CH_3I (99%), *n*-C_3H_7I (99%), *n*-C_4H_9I (99%), and *cyclo*-$C_6H_{11}I$ (98%) were obtained from Sigma Aldrich Japan. C_2H_5I (99%), toluene (99%), durene (98%), and *p*-$CH_3C_6H_4I$ (95%) were obtained from Wako Pure Chemicals. All reagents (except for *p*-$CH_3C_6H_4I$ and durene) were subjected to freeze−pump−thaw cycling before use. Cl_2 (high-purity grade, Sumitomo Seika), N_2 (99.999%, Teisan), and O_2 (>99.995%, Teisan) were used without further purification.

3. Results and Discussion

3.1 $C_nH_{2n+1}I-Cl$ Adducts. Optical absorption appeared at 440−520 nm following flash photolysis of the $C_nH_{2n+1}I/Cl_2/N_2$ mixtures at 355 nm. Figure 1 shows a typical decay profile of the absorption intensity at 440 nm for the product from the reaction of C_3H_7I + Cl at 263 K, with and without O_2. The decay is caused by the diffusion of the products from the observation region because abstraction reaction 1b can be neglected at this temperature as will be described below. Under 100 Torr of O_2, there was no discernible effect on the temporal decay profiles for all compounds we used here. These results indicate that the observed absorption is attributable to adducts and not to $C_nH_{2n}I$ radicals that may be produced via the abstraction reaction 1b, because these radicals are rapidly consumed by the reaction with O_2.[15,16]

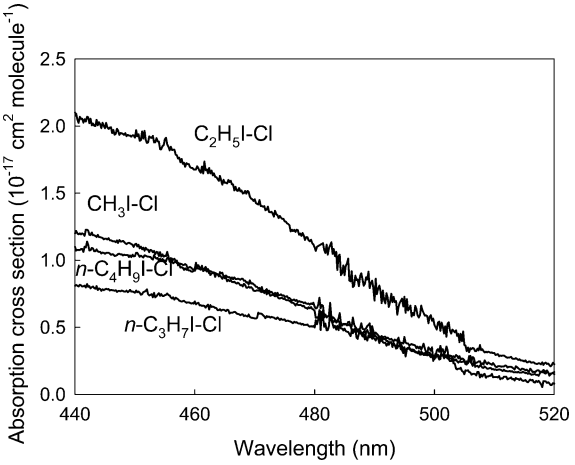

Figure 2. Absorption spectra of $C_nH_{2n+1}I-Cl$ at 263 K with 100 Torr of N_2 diluent.

Figure 2 shows the absorption spectra of the products from the reactions of $C_nH_{2n+1}I$ + Cl at 263 K and 100 Torr of N_2 diluent. There was no discernible structure in the spectra. As will be described below, the electronic transition energies and oscillator strengths are theoretically calculated (Table 1). The variation of the cross sections for compounds with different alkyl chain seems not to relate with these calculated results. Information on potential energy surfaces of ground and excited states is needed to explain absorption intensities in their wing region. The observed absorbance at 440 nm following flash photolysis of the $C_nH_{2n+1}I/Cl_2/N_2$ mixture was measured at the maximum concentration (typically about 50-μs delay) as a function of temperature over the range 250−320 K in 100 Torr N_2 diluent. The absorption was normalized to that observed at 250 K in Figure 3. The absorption attributable to adduct $C_nH_{2n+1}I-Cl$ decreases almost linearly with temperature because of back reaction (−1a) and the hydrogen abstraction reaction 1b. If the abstraction rate and equilibrium constants are reported, the temperature dependence of the CH_3I-Cl formation is well reproduced for CH_3I.[10] However, since these data are not available for higher RI compounds, the temperature dependence is not simulated. According to our previous results for CH_3I,[10] we could assume that the absorption spectra of $C_nH_{2n+1}I-Cl$ do not change significantly over the present temperature range. If this is the case for other compounds, the present decrease in absorbance at 440 nm with temperature reflects the fact that the adduct yield decreases with temperature. In Figure 3, we define here the "adduct stabilization temperature". That is the critical temperature, below which the adduct formation path becomes the sole reaction pathway for the reaction of $C_nH_{2n+1}I$ + Cl. On the basis of the measured initial Cl atom concentration, the absolute absorption cross sections are estimated with use of eq III. We plot the adduct stabilization temperature versus ionization potential of the parent compounds. A liner relationship in Figure 4 is evidence for the CT complex formation.

The *x*-intercepts of Figure 3 are extrapolated to 360, 370, 367, and 351 K (error bars are ±10 K) for CH_3I, C_2H_5I, *n*-C_3H_7I, and *n*-C_4H_9I, respectively. These temperatures are defined here as "adduct decomposition temperature", above which no apparent adduct formation occurs. For CH_3I-Cl, Ayhens et al.[8] reported no adduct formation was observed at 364 K, which is consistent with our results. We also observed the absorption of the adduct, *cyclo*-$C_6H_{11}I-Cl$. Results of the adduct formation are summarized in Table 1.

Because the decay signals started even at <50 μs, the reaction rate constants of C_2H_5I, C_3H_7I, and C_4H_9I with Cl at 263 K are

TABLE 1: Absorption Cross Sections and Formation Temperatures of the Adducts, RI−Cl

compounds	ionization potential of RI (eV)	cross section at 440 nm (10^{-17} cm^2)	adduct stabilization temperature (K)[a]	theoretical bond energy (kJ mol^{-1})	theoretical peak wavelength (nm) (oscillator strength)	references
CH_3I	9.5	1.2	250	59.0	339 (0.18)	10
C_2H_5I	9.4	2.1	259	61.7	342 (0.16)	10
n-C_3H_7I	9.3	0.81	273	61.2		c
n-C_4H_9I	9.2	1.1	283	62.0	345 (0.17)	c
C_6H_5I	8.7	>3.7	b	56.5	459 (0.14)	c
C_6F_5I	9.5	>0.49	b			c
p-$CH_3C_6H_4I$	8.6	>0.86	b			c
cyclo-$C_6H_{11}I$	8.9	>0.78	b			c

[a] Adduct stabilization temperature is the critical temperature below which the adduct formation path becomes the sole reaction pathway for RI + Cl. [b] No apparent adduct stabilization temperature was observed. [c] This work.

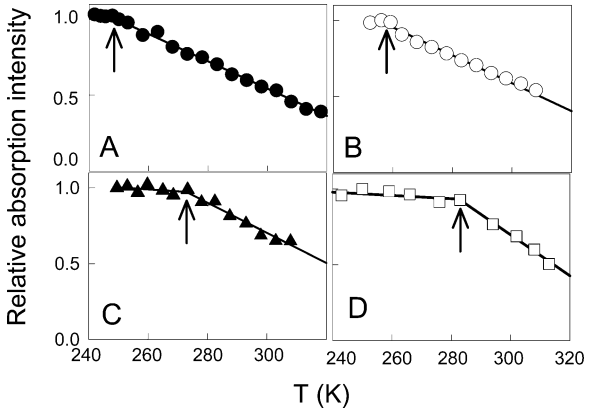

Figure 3. Temperature dependence of relative absorption intensity of $C_nH_{2n+1}I-Cl$. $n = 1$ (A), $n = 2$ (B), $n = 3$ (C), and $n = 4$ (D). Adduct stabilization temperatures are shown by the arrows.

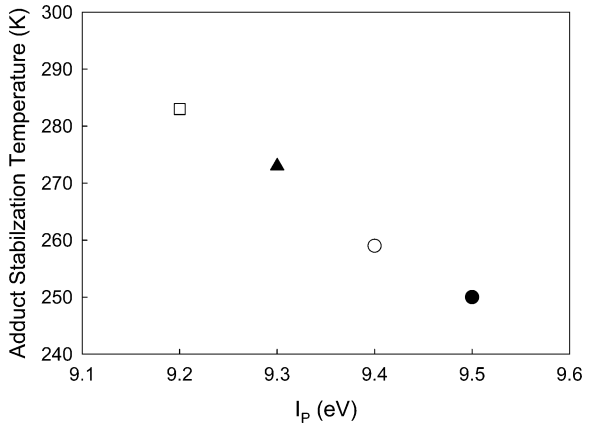

Figure 4. Adduct stabilization temperatures vs ionization potentials of parent molecules, $C_nH_{2n+1}I$; $n = 1$ (closed circle), $n = 2$ (open circle), $n = 3$ (triangle), and $n = 4$ (square).

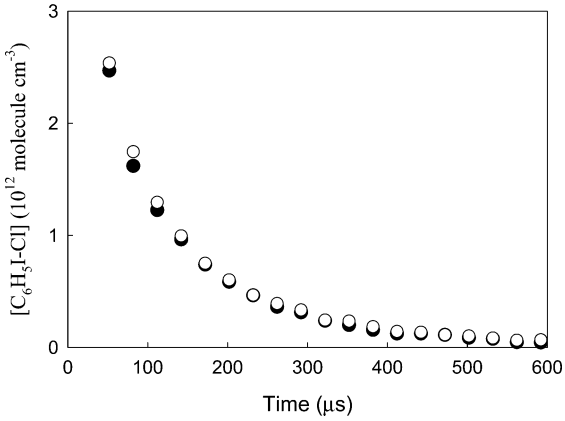

Figure 5. Typical decay time profiles of C_6H_5I-Cl at 263 K with 100 Torr of N_2 diluent (closed circle) or 100 Torr of O_2 diluent (open circle).

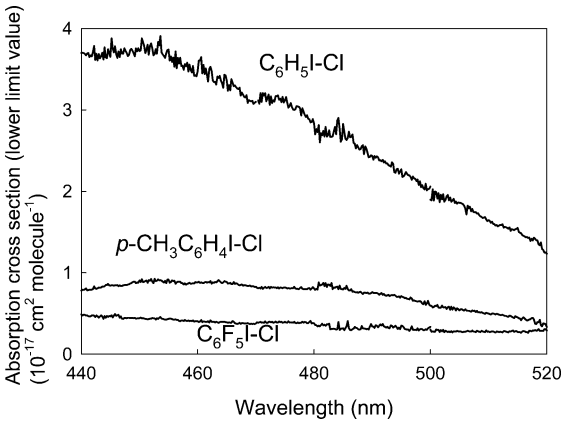

Figure 6. Absorption spectra of C_6H_5I-Cl, C_6F_5I-Cl, and *p*-$CH_3C_6H_4I-Cl$ at 263 K with 100 Torr of N_2 diluent. These absorption cross sections are lower limit value.

larger than that for CH_3I with Cl (2.1×10^{-11} cm^3 molecule^{-1} s^{-1} at 250 K).[10] However, those rate constants could not be determined because we could not measure the rise curves below 50 μs because of strong scattered light from the photolysis laser.

3.2 C_6H_5I-Cl, C_6F_5I-Cl, and *p*-$CH_3C_6H_4I-Cl$. Figure 5 shows a typical temporal decay profile of the adduct, C_6H_5I-Cl. Addition of O_2 had no effect on the decay profile. The decay of adduct signals was caused by mainly the diffusion from the detection region and possibly the halogen substitution reaction. The H-atom abstraction from the CH_3 group could be included for *p*-$CH_3C_6H_4I$. The absorption spectra of C_6H_5I-Cl, C_6F_5I-Cl, and *p*-$CH_3C_6H_4I-Cl$ between 440 and 520 nm are shown in Figure 6. No discernible structure in the spectra was observed. No CT complex signal for toluene + Cl and durene + Cl was observed at 440 nm. The temperature dependence on the formation of those adducts is shown in Figure 7. The adduct stabilization temperature is not clearly seen in Figure 7. Since the vapor pressure of C_6F_5I becomes very low below 270 K, it was difficult to conduct experiments with C_6F_5I. Since the adduct stabilization temperature was not obtained, we estimated the lower limits of the absolute cross sections with the use of eq II and the measured initial Cl atom concentration.

The absorption intensity of the C_6H_5I-Cl adduct at 440 nm monotonically decreases with temperature. The sharp decrease of *p*-$CH_3C_6H_4I-Cl$ is possibly due to the H-abstraction reaction at the methyl group. Since the temperature dependence curve for C_6H_5I-Cl has almost the same slope as for C_6F_5I-Cl in Figure 7, the abstraction reaction of H atom would not occur in the reaction of C_6H_5I + Cl. Instead, the substitution reaction occurs over this temperature range. The substitution reaction

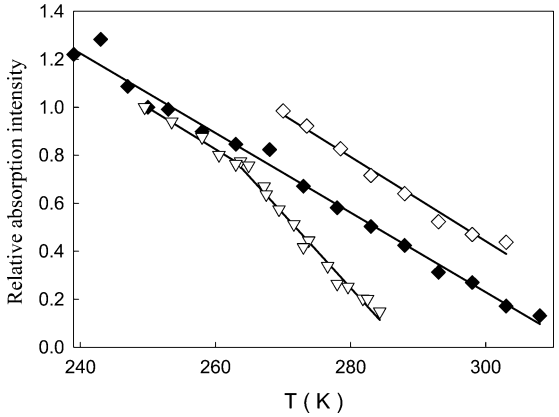

Figure 7. Temperature dependence of relative absorption intensities of C_6H_5I-Cl (closed diamond, normalized at 250 K), C_6F_5I-Cl (open diamond, normalized at 270 K), and *p*-$CH_3C_6H_4I-Cl$ (triangle, normalized at 250 K) with 100 Torr of N_2 diluent.

of C_6H_5I with Cl at room temperature was reported by Andersen et al.[17] They suggested the adduct formation followed by substitution reaction with unit yield.

$$C_6H_5I + Cl \rightleftarrows C_6H_5I-Cl \quad (2a)$$

$$C_6H_5I\text{-}Cl \rightarrow C_6H_5Cl + I \quad (3)$$

We conclude that the absorption decrease of C_6H_5I-Cl with temperature is due to the reverse reaction and the substitution reaction. The *x*-intercepts of Figure 7, the adduct decomposition temperatures, are 314, 325, and 288 K (±10 K) for C_6H_5I, C_6F_5I, and *p*-$CH_3C_6H_4I$, respectively.

We could not observe any CT complex signal in the C_6H_5Br + Cl reaction at two different wavelengths, 440 and 520 nm, for 243 K under 100 Torr of total pressure of N_2 diluent. These results could be explained by the bond strength of $RBr-Cl$ being about half of $RI-Cl$ as shown by our theoretical calculations below, that is, the bond dissociation energy in C_6H_5Br-Cl adduct is 37.3 kJ mol^{-1} while 56.5 kJ mol^{-1} in C_6H_5I-Cl and about 60 kJ mol^{-1} in $C_nH_{2n+1}I-Cl$. We previously reported no formation of CH_3Br-Cl adducts above 213 K.[10] Piety et al.[9] reported that the bond energy of CH_3Br-Cl is 25. 6 kJ mol^{-1} and that the CH_3Br-Cl adduct formation occurs only below 177 K.

4. Theoretical Calculations

All calculations were carried out using the Gaussian 03 revision B.04 program packages.[19] The equilibrium geometries of the ground state of the C_4H_9I-Cl and C_6H_5I-Cl adducts were optimized employing a hybrid density functional theory, B3LYP, on the basis of Becke's three-parameter nonlocal exchange functional[20−22] with nonlocal correction functional of Lee, Yang, and Parr.[23] A 6-311++G(d,p) basis set was used for carbon, hydrogen, chlorine, and bromine, while a 6-311G-(d,p) basis set was used for iodine. Electronic transitions of the adducts were investigated employing time-dependent density functional theory (TD-DFT) calculations.[24] The calculations were based on the $^2A'$ ground-state equilibrium.[25] In the present calculation of the vertical excitation energies, C_s molecular symmetry was assumed for the equilibrium geometry of the ground state that is shown in supplement Figures 1 and 2. The C−I−Cl bond angles for the C_4H_9I-Cl adduct is 84.2°. This angle is close to those of CH_3I-Cl (84.6°) and C_2H_5I-Cl (83.6°). The C−I−Cl bond angle for the C_6H_5I-Cl adduct is 98.5°. The Cl−I bond length of C_4H_9I-Cl is 2.901 Å, which is close to the Cl−I bond length of CH_3I-Cl (2.907 Å) and C_2H_5I-Cl (2.901 Å). For C_6H_5I-Cl adduct, the bond length is 2.926 Å. Detailed structures are shown in supplement Table 1.

For alkyl adducts, $C_nH_{2n+1}I-Cl$, the trans form is more stable than the cis form by 3.8, 3.0, and 3.2 kJ mol^{-1} for $n = 2$, 3, and 4, respectively. For C_6H_5I-Cl, the Cl atom is localized around I atom, and the I−Cl bond energy of the plane-structured C_6H_5I-Cl is 54.9 kJ mol^{-1}. The energy difference between the out-of-plane and the in-plane isomer is only 1.6 kJ mol^{-1}. Therefore, the Cl atom would act as a free rotator in the adduct.

The theoretically determined I−Cl bond energies for *n*-C_3H_7I-Cl, *n*-C_4H_9I-Cl, and C_6H_5I-Cl are 61.2, 62.0, and 56.5 kJ mol^{-1}, respectively (Table 1), while the theoretically I−Cl bond strength for CH_3I-Cl and C_2H_5I-Cl were previously determined to be 59.0 and 61.7 kJ mol^{-1}, respectively.[10] The value for CH_3I-Cl is in good agreement with the previously reported theoretical calculation, 59.3 kJ mol^{-1}, by Ayhens et al.[8] There is an apparent difference between $C_nH_{2n+1}I-Cl$ and C_6H_5I-Cl in the bond energies, because of the steric effect between the benzene ring and the Cl atom. Indeed, the C−I−Cl bond angle of the C_6H_5I-Cl adduct is wider than that of the $C_nH_{2n+1}I-Cl$ adduct. The Cl−I bond length in C_6H_5I-Cl is also longer than that in $C_nH_{2n+1}I-Cl$. Furthermore, the HOMO extends over the benzene moiety in theses compounds, which reduces the orbital overlap and leads to a smaller binding energy even though the I_P is lower for iodobenzene.

The bond energy could be correlated with experimentally determined adduct decomposition temperature. Our results show that the theoretical bond energies have no appreciable differences among $C_nH_{2n+1}I-Cl$ adducts. The decomposition temperatures also have no appreciable differences among $C_nH_{2n+1}I-Cl$ adducts.

For *n*-C_4H_9I-Cl, our calculations suggest that a strong absorption band appears at 344 nm, with an oscillator strength $f = 0.17$ (Table 1 and supplement Table 2). This transition may be assigned to a $\sigma-\sigma^*$ transition localized on the I−Cl bond. The absorption observed in the present experiment is attributable to the red wing of this transition. These results are consistent with previous reports for CH_3I-Cl and C_2H_5I-Cl.[10] All adduct absorptions of $C_nH_{2n+1}I-Cl$ in the visible region are assigned to be the red wing of the $\sigma-\sigma^*$ transition.

For C_6H_5I-Cl, our calculations suggest that a strong absorption band appears at 458 nm with $f = 0.14$ (Table 1 and supplement Table 2). This transition is assigned to a $\sigma-\sigma^*$ transition localized on the I−Cl bond. The strong absorption observed experimentally at around 450 nm is attributable to the peak of the $\sigma-\sigma^*$ transition. The bond dissociation energy of the I−Cl bond is 56.5 kJ mol^{-1}.

For C_6H_5Br-Cl, our calculations suggest that a strong absorption band appears at 533.71 nm with $f = 0.1571$ (supplement Table 2). The bond dissociation energy of the Br−Cl bond is 37.3 kJ mol^{-1}.

5. Conclusion

We have observed new absorption bands of the I−Cl adducts in the reaction of aliphatic and aromatic iodides with Cl atoms. Adduct stabilization temperatures correlated well with ionization potentials of the iodo-compounds. None of these adducts react with O_2 at 263 K. The absorption spectra of the adducts are assigned to the $\sigma-\sigma^*$ transitions localized on the I−Cl bond, on the basis of the present theoretical calculations. These results indicate that the observed adducts are ascribable to CT complexes.

Acknowledgment. The authors are grateful to Dr. N. Kanno of the University of Tokyo for his help in theoretical calculations. The authors also thank Prof. S. Aloisio of California State University for helpful discussion. This work is partly supported by a grant from the 21st Century COE project of Kyoto University.

Supporting Information Available: Tables and figures of calculated optimized geometries and a table of electronic transition energies and oscillator strengths. These materials are available free of charge via the Internet at http://pubs.acs.org.

References and Notes

(1) Carpenter, L. J. *Chem. Rev.* **2003**, *103*, 49.

(2) Saiz-Lopez, A.; Plane, J. M. C. *Geophy. Res. Lett*. **2004**, *31*, L04112.

(3) Calvert, J. G.; Lindberg, S. E. *Atoms. Environ*. **2004**, *38*, 5087.

(4) Kanaya, Y.; Akimoto, H. *Chem. Rec.* **2002**, *2*, 199.

(5) Burkholder, J. B.; Curtius, J.; Ravishankara, A. R.; Lovejoy, E. R. *Atoms. Phys. Chem*. **2004**, *4*, 19.

(6) O'Dowd, C. D.; Jimenez, J. L.; Bahreini, R.; Flagan, R. C.; Seinfeld, J. H.; Kulmala, M.; Pirjola, L.; Hoffmann, T. *Nature* **2002**, *417*, 632.

(7) Bilde, M.; Sehested, J.; Mogelberg, T. E.; Wallington, T. J.; Nielsen, O. J. *J. Phys. Chem.* **1996**, *100*, 7050.

(8) Ayhens, Y. V.; Nicovich, J. M.; McKee, M. L.; Wine, P. H. *J. Phys. Chem. A* **1997**, *101*, 9382.

(9) Piety, C. A.; Soller, R.; Nicovich, J. M.; McKee, M. L.; Wine, P. H. *Chem. Phys*. **1998**, *231*, 155.

(10) Enami, S.; Hashimoto, S.; Kawasaki, M.; Nakano, Y.; Ishiwata, T.; Tonokura, K.; Wallington, T. J. *J. Phys. Chem. A* **2005**, *109*, 1587.

(11) O'Keefe, A.; Deacon, D. A. G. *Rev. Sci. Instrum*. **1988**, *59*, 2544.

(12) Yu, T.; Lin, M. C. *J. Am. Chem. Soc.* **1993**, *115*, 4371.

(13) Wheeler, M. D.; Newman, S. M.; Orr-Ewing, A. J.; Ashfold, M. N. R. *J. Chem. Soc., Faraday. Trans.* **1998**, *94*, 337.

(14) Berden, G.; Peeters, R.; Meijer, G. *Int. Rev. Phys. Chem.* **2000**, *19*, 565.

(15) Sander, S. P.; Friedl, R. R.; Ravishankara, A. R.; Golden, D. M.; Kolb, C. E.; Kurylo, M. J.; Huie, R. E.; Orkin, V. L.; Molina, M. J.; Moortgat, G. K.; Finlayson-Pitts, B. J. *Chemical Kinetics and Photochemical Data for Use in Stratospheric Modeling*, Evaluation 14; Jet Propulsion Laboratory, NASA: California, 2003.

(16) Enami, S.; Ueda, J.; Goto, M.; Nakano, Y.; Aloisio, S.; Hashimoto, S.; Kawasaki, M. *J. Phys. Chem. A* **2004**, *108*, 6347.

(17) Andersen, M. P. S.; Ponomarev, D. A.; Nielsen, O. J.; Hurley, M. D.; Wallington, T. J. *Chem. Phys. Lett.* **2001**, *350*, 423.

(18) *NIST Chemistry Webbook, Standard Reference Database* vol. 69.

(19) Frisch, M. J.; Trucks, G. W.; Schlegel, H. B.; Scuseria, G. E.; Robb, M. A.; Cheeseman, J. R.; Montgomery, J. A., Jr.; Vreven, T.; Kudin, K. N.; Burant, J. C.; Millam, J. M.; Iyengar, S. S.; Tomasi, J.; Barone, V.; Mennucci, B.; Cossi, M.; Scalmani, G.; Rega, N.; Petersson, G. A.; Nakatsuji, H.; Hada, M.; Ehara, M.; Toyota, K.; Fukuda, R.; Hasegawa, J.; Ishida, M.; Nakajima, T.; Honda, Y.; Kitao, O.; Nakai, H.; Klene, M.; Li, X.; Knox, J. E.; Hratchian, H. P.; Cross, J. B.; Adamo, C.; Jaramillo, J.; Gomperts, R.; Stratmann, R. E.; Yazyev, O.; Austin, A. J.; Cammi, R.; Pomelli, C.; Ochterski, J. W.; Ayala, P. Y.; Morokuma, K.; Voth, G. A.; Salvador, P.; Dannenberg, J. J.; Zakrzewski, V. G.; Dapprich, S.; Daniels, A. D.; Strain, M. C.; Farkas, O.; Malick, D. K.; Rabuck, A. D.; Raghavachari, K.; Foresman, J. B.; Ortiz, J. V.; Cui, Q.; Baboul, A. G.; Clifford, S.; Cioslowski, J.; Stefanov, B. B.; Liu, G.; Liashenko, A.; Piskorz, P.; Komaromi, I.; Martin, R. L.; Fox, D. J.; Keith, T.; Al-Laham, M. A.; Peng, C. Y.; Nanayakkara, A.; Challacombe, M.; Gill, P. M. W.; Johnson, B.; Chen, W.; Wong, M. W.; Gonzalez, C.; Pople, J. A. Gaussian, Inc.: Pittsburgh, PA, 2003.

(20) Becke, A. D. *J. Chem. Phys.* **1993**, *98*, 5648.

(21) Becke, A. D. *J. Chem. Phys.* **1992**, *97*, 2155.

(22) Becke, A. D. *J. Chem. Phys.* **1992**, *97*, 9173.

(23) Lee, C.; Yang, W.; Parr, R. G. *Phys. Rev. B* **1988**, *37*, 785.

(24) Koch, W.; Holthausen, M. C. *A Chemist's Guide to Density Functional Theory*; Wiley-VCH: Weinheim, Germany, 2000.

(25) Hirata, S.; Head-Gordon, M. *Chem. Phys. Lett.* **1999**, *302*, 375.